Improved conflat cell for repeatable electrochemical testing to 400°C

Fleischauer, Michael D.; Kupsta, Martin R.; Johnson, Aliesha D.

Publisher's version / Version de l'éditeur:
https://doi.org/10.1149/2.0201902jes
Journal of The Electrochemical Society, 166, 2, pp. A398-A402, 2019-02-01

Improved Conflat Cell for Repeatable Electrochemical Testing to 400°C

Michael D. Fleischauer,[1,2,*,z] **Martin R. Kupsta,**[2] **and Aliesha D. Johnson**[1,3]

[1]*National Research Council - Nanotechnology Research Centre, Edmonton, AB T6G 2M9, Canada*
[2]*Department of Physics, University of Alberta, Edmonton, AB T6G 2E1, Canada*
[3]*Department of Chemical and Materials Engineering, University of Alberta, Edmonton, AB T6G 1H9, Canada*

Reusable electrochemical cells that can remain hermetically sealed to 400°C using commercially available and easy-to-machine components are described. Unlike most other cell designs, cell sealing and electrode electrical isolation are decoupled, allowing for consistent, low cost testing (~$2 in parts per cell rebuild) in a wide range of environments. Additional functionality (e.g. windows, valving, sensors) can be incorporated without compromising cell performance. Examples using these improved Conflat cells for extended room temperature testing and investigations of electrode phase transitions and accelerated electrolyte breakdown at elevated temperatures are provided.

 [DOI: 10.1149/2.0201902jes]

Manuscript submitted November 5, 2018; revised manuscript received December 21, 2018. Published February 1, 2019.

Lithium-ion rechargeable batteries are the dominant reusable energy storage technology because of their performance and ease of use, but safety and cost challenges persist. High profile fires triggered by lithium-ion batteries highlight safety challenges in everyday use,[1] and reflect the unsuitability of current lithium-ion technology for a number of high value, harsh (e.g. high temperature) environments from outer space to deep underground. Many applications require operation well above 100°C.[2,3] Standard electrochemical test hardware is unsuited to testing at high temperatures (above 60−80°C).[4] Here we describe important improvements in cell design to enable reliable electrochemical testing over a wide temperature range (up to 400°C).

Coin cells are a common lithium-ion electrode and electrolyte material test platform.[5] Coin cell sealing is achieved by plastically deforming a polyethylene or polypropylene gasket. Gasket softening limits the use of coin cells to below ca. 80°C for most electrolyte solvents, or lower with volatile solvents such as tetrahydrofuran.[6] Alternative gasket materials may offer slight sealing improvements at higher temperatures.[7] Other approaches include embedding coin cells within a high-temperature compatible epoxy.[8] However, coin cells can deform with high internal pressure[6] and can be challenging to use with in-situ techniques[9] and in three-electrode designs.[10]

Swagelok cells offer more experimental flexibility as the sealing ferrules and cell body are available in a variety of materials (e.g. stainless steel, PTFE[11]), and many different styles of connectors (e.g. unions for two electrode measurements, tees for three electrode measurements[12]) and adapters (e.g. for gas monitoring[13]) are commercially available. However, electrical isolation between electrodes requires either a plastic cell body or plastic-coated plungers, and higher temperature testing is limited to 55°C.[12,14] PTFE also reacts with lithium at low voltages, a major issue when investigating negative electrode materials.[6] Swagelok cells incorporating metal plungers embedded in alumina[15] were successfully cycled at 100 and 150°C.[16,17] However, mismatched thermal expansion coefficients between the metal body, alumina sleeves, and metal plungers can limit cell sealing performance at higher temperatures.

Conflat-style flanges can be used to achieve ultra-high vacuum tight seals by impinging opposing knife edges in to a softer gasket material. Conflat-style electrochemical test cells using stainless steel flanges and PTFE gaskets were successfully demonstrated at 200°C;[6] low voltage electrode materials were investigated using a custom-machined flange separating the PTFE gaskets from the electrodes and electrolyte. Additional PTFE was required between the steel flanges to ensure electrical isolation, preventing full impingement of the knife edges and complete sealing of the cell. PTFE also softens considerably at temperatures above 200°C. Commercial high-temperature compatible designs incorporating other plastics (e.g. PEEK) are also limited to 200°C.[18,19]

All cell designs described above use the cell gasket for two purposes - cell sealing, and electrical isolation. A modified Conflat-style cell intended for molten sodium electrode cells used copper gaskets for cell sealing and commercial ultra-high vacuum compatible feedthroughs for electrical isolation.[20] Such a cell design can operate at temperatures up to 300°C but lacks the ability to apply (or control) stack pressure (typically 0.1–1 MPa normal to the electrode surface, to mimic a tightly wound and tightly packed commercial cell).[21]

Here we present an improved Conflat cell design that decouples cell sealing and electrical isolation without compromising stack pressure or cell performance. Glass-to-metal seals are the commercial standard for primary high-temperature compatible cells (e.g. Li/$SOCl_2$ cells for down-hole tools). Glass-to-metal Conflat adapters are commercially available, can be used to maintain an ultra-high vacuum tight seal to 415°C, and are compatible with aggressive electrolytes and low and high voltage electrode materials. Furthermore, a wide range of vacuum-tight accessories are available (including Conflat to Swagelok adapters). Glass-to-metal Conflat cell performance at room and higher temperatures is described below.

Experimental

Double-ended glass-to-metal Conflat adapters are the core component of the improved Conflat cell described here. A schematic of an adapter and all other cell components is provided in Figure 1. Double-ended adapters were purchased from Larson Electronic Glass (Redwood City, CA USA). All adapters consisted of two 54 mm (2-1/8") Conflat half nipples bonded together via a nominal 25 mm long glass section. The inner diameter of the glass varied from adapter to adapter between 21 mm and 23 mm. Two metal/glass combinations with matched thermal expansion coefficients in a wide variety of adapter lengths and diameters are available. The maximum operating temperature is limited by the mechanical properties of the glass, glass-to-metal bonds, and gaskets.

Conflat flanges and the corresponding copper gaskets were purchased from Nor-Cal Products, Inc. (Yreka, CA USA). Flanges were sealed by impinging the Conflat knife edges into the gasket until the flange edges were in uniform mechanical contact. Flange sealing was performed using 1/4"-28 bolts and plate nuts (MDC Vacuum Products LLC, Hayward, CA USA). Anti-seize tape (McMaster-Carr, Aurora, OH USA) was applied to the bolts prior to assembly for cells operated

*Electrochemical Society Member.
[z]E-mail: michael.fleischauer@nrc.ca

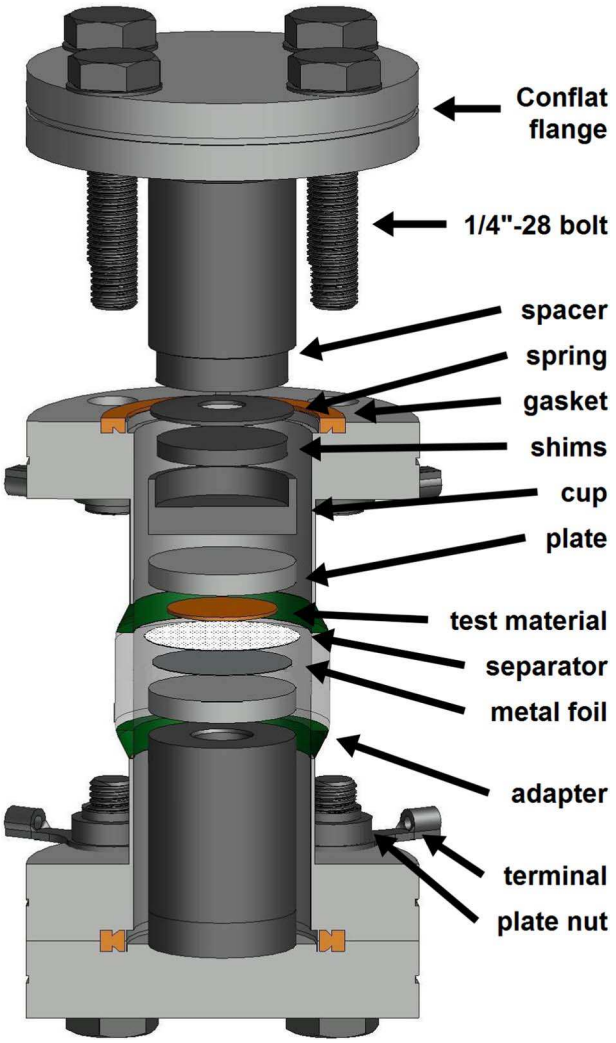

Figure 1. Exploded view of the cell assembly. Components are labeled and described in the text.

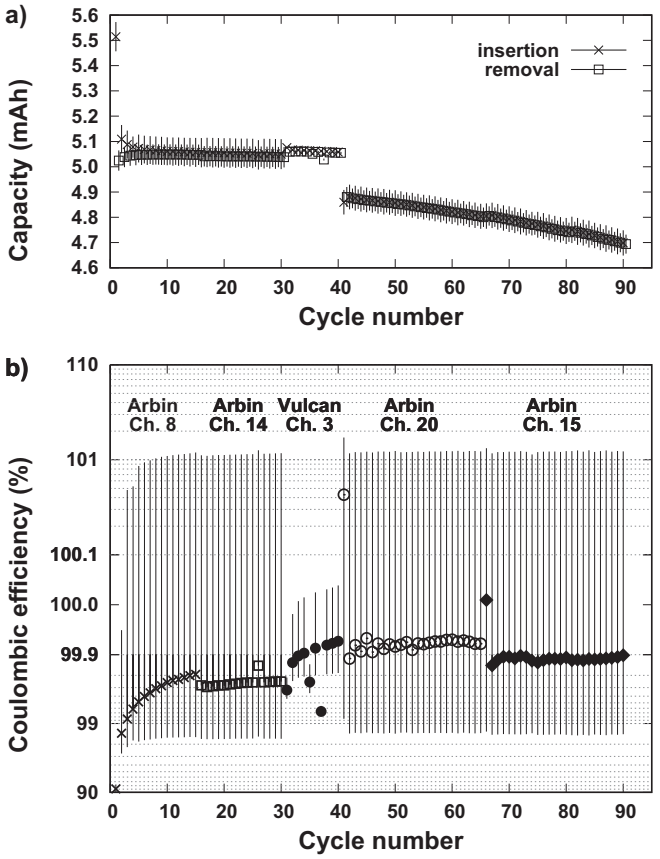

Figure 2. a) Capacity and b) coulombic efficiency of a lithium/graphite Conflat cell as a function of cycle number. Instrument and channel numbers are indicated.

above room temperature. Uninsulated crimp ring terminals (Digikey, Thief River Falls, MN USA) were placed between plate nuts and the inner flange face to ease connection with alligator-clip terminated wires. One end of each adapter was wrapped in electrically insulating fiberglass tape (McMaster-Carr) for ease of handling on conductive surfaces.

Internal cell components - a series of rigid stainless steel parts, a Belleville spring, electrodes, and a separator - are shown in Figure 1. This configuration is the same as standard coin cells but adapted to the longer double-ended adapters. As there is a fixed distance between the flanges when sealed, one can adjust the compression of the Belleville spring by incorporating shims. Shims were selected such that the Belleville spring was compressed by 0.254 mm (0.010"), corresponding to a stack pressure of 0.8 MPa. Spring compression was determined using feeler gauges between the adapter body and top flange, and controlled within ~15 μm (0.0005"). Shims and spring were constrained in custom machined cups for alignment and ease of assembly.

All cells were assembled upright in an Ar-filled glove box maintained at <5 ppm H_2O and O_2. Li electrodes were punched from brushed 0.102 mm (0.004") thick lithium foil (Rockwood Lithium, Charlotte, NC USA). Whatman GF/A glass filters (Fisher Scientific, Hampton, NH USA) were baked at 400°C for 24 hours under flowing argon, and stored in the glove box prior to use. Electrolyte was introduced in two stages with 100 μL aliquoted below and above the separator. When required, electrolyte was incorporated into the separator by momentarily evacuating the cell using a Conflat-to-Swagelok flange, rubber Conflat gasket, a three-way valve, and the glove box roughing pump. This method allows for direct control of the amount of electrolyte in the cell, which can be important for quantifying electrolyte breakdown.

Graphite electrodes were purchased from MTI Corp. (Richmond, CA USA) and cycled using 1 M $LiPF_6$ (battery grade, Sigma-Aldrich, St. Louis, MO USA) in ethylene carbonate (EC, 99%, Aldrich): diethyl carbonate (DEC, 99%, Alfa-Aesar, Ward Hill, MA USA) 1:2 vol.:vol. electrolyte. 500 nm thick Al films were sputter-deposited on to 16 mm dia. stainless steel spacers (MTI Corp.) and cycled using 1 M $LiClO_4$ in EC:DEC 1:2 vol.:vol. or 1 M $LiN(SO_2CF_3)_2$ in EC : propylene carbonate (PC, 99.7%, Aldrich) 1:1 vol.:vol. electrolyte. 200 nm thick sputter-deposited Si films were cycled using 1 M $LiN(SO_2CF_3)_2$ in EC:PC 1:1 vol.:vol. electrolyte.

Electrochemical cycling was performed on two systems: an Arbin MSTAT multichannel potentiostat with an incubator (Fisher) maintained at 25 ± 0.5°C, or at higher temperatures using a lab-built multichannel system ("Vulcan") with channel-dependent temperature control. All cells were tested on their side (with both ends of the Conflat cell being supported by the heater). Vertical operation (as shown in Figure 1, only one end supported by the heater) may further improve electrolyte retention and cell performance. Cell temperatures were verified by embedding a 1000 Ω Resistance Temperature Detector (RTD, Heraeus Sensor Technology, Hanau, Germany) within a ceramic washer, replacing the active cell components with the RTD assembly, and measuring the overall cell resistance as a function of heater temperature.

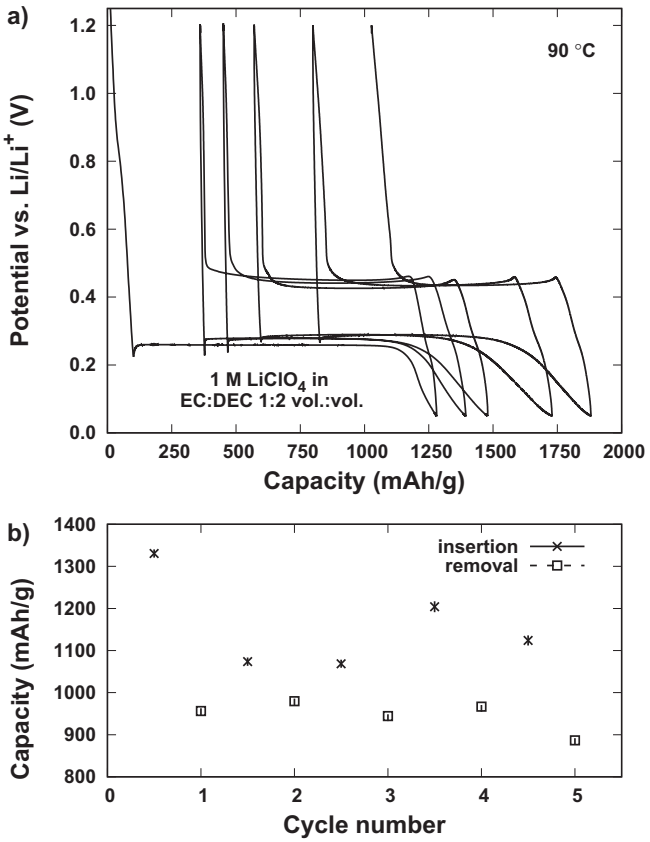

Figure 3. a) Potential vs. capacity and b) capacity vs. cycle number for a Li-Al Conflat cell cycled at 90°C. Cell electrolyte is indicated.

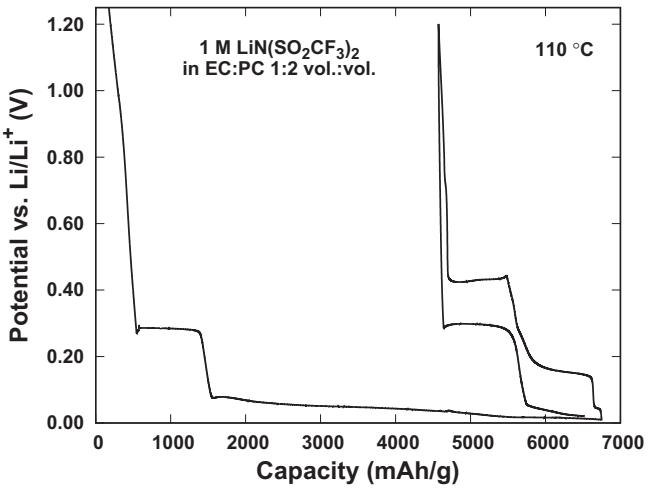

Figure 4. Potential vs. capacity data from a Li-Al Conflat cell cycled at 110°C. Cell electrolyte is indicated.

Results and Discussion

Results from a Conflat cell with lithium and graphite electrodes cycled near room temperature are provided in Figure 2. Cycles were performed between 1.2 V and 5 mV vs. Li metal at a rate of C/10 with a two-step trickle charge (C/20, C/40) on lithium insertion at 25°C (cycles 1-30) or 30°C (cycles 31–40). Cycles 41-90 were performed at a rate of C/10 without trickle steps at 25°C. In total, cycles 1–90 were performed over the course of 91 days. After a few cycles, cell capacity was nearly constant at 5.05 mAh for the first 40 cycles (see Figure 2a). Eliminating the trickle insertion steps reduced cell capacity from 5.05 mAh to 4.85 mAh. Cell capacity subsequently faded by less than 0.1% per cycle after cycle 40. After more than 300 days of storage in the lab, additional cycling at a rate of C/20 led to a capacity of 4.8 mAh.

Coulombic efficiency data corresponding to the capacity data shown in Figure 2a) is provided as Figure 2b). Coulombic efficiency (CE) values are shown on a log-linear-log scale to highlight the region of interest (i.e. close to 100%).[22] Almost all CE values are between 99.7–99.95%, and within experimental uncertainty of unity. CE values outside of this range after the first few cycles are due to switching the cell between instrument channels. CE values also match capacity retention values (~99.9% per cycle) over cycles 40–90. These CE values are better than the 99.8% CE reported for similar coin cells and 99.7% for similar Conflat cells sealed using (only low temperature compatible) HDPE gaskets.[6] Here, CE measurement resolution is limited by uncertainty in test instrument current measurement; CE values are limited by material performance, not by the cell. No effort to optimize electrolyte composition, volume, or stack pressure was made. Glass-to-metal Conflat cells with copper gaskets perform at least as well as coin cells at room temperature, and can also operate at higher temperatures.

Results from a lithium-aluminum cell cycled at 90°C are provided in Figure 3. Cycling was performed between 1.2 V and 50 mV at a rate of C/5 for cycles 1–2.5 and at a rate of C/30 for cycles 2.5–5. Potential vs. capacity data shown in Figure 3a) is dominated by flat plateaus on lithium insertion and removal associated with the Li + Al ↔ LiAl phase transition commonly observed at room temperature and expected from the equilibrium phase diagram.[23] Reversible formation of LiAl corresponds to a capacity of 990 mAh/g. Lithium insertion and removal capacities corresponding to the data shown in Figure 3a) are provided in Figure 3b). Lithium insertion capacities start to plateau at ca. 1070 mAh/g before increasing to 1200 mAh/g when the cycling rate decreases (and the duration of each cycle increases). Lithium removal capacities are within 50 mAh/g of the expected value. Insertion capacities above 1000 mAh/g can likely be attributed to Li consumption due to solid-electrolyte interphase (SEI) formation. Changes in the potential vs. capacity data shown in Figure 3a) above 0.5 V suggest a small but increasing amount of lithium is being removed from previously inaccessible/non-existent sites; changes below 0.2 V suggest increasingly sluggish kinetics, even at 90°C. Both changes are consistent with the growth of non-trivial SEI layer.

Results from a lithium-aluminum cell cycled at 110°C between 1.2 V and 10 mV vs. Li metal at a nominal rate of C/30 are provided in Figure 4. Two things are immediately apparent. First, the insertion capacity has increased dramatically, to almost 7,000 mAh/g. Second, at least two plateaus on insertion and three plateaus on removal are apparent. New reactions (in addition to Li + Al ↔ LiAl) are occurring at potentials below 200 mV. The equilibrium Li-Al phase diagram contains multiple Li-Al phases (LiAl, Li_3Al_2, Li_9Al_4). Electrochemical formation of Li_3Al_2 and Li_9Al_4 has only been observed above 400°C using molten salt electrolytes;[24] slow diffusion is thought to inhibit their formation at room temperature.[25] The total lithium removal capacity of ~2200 mAh/g corresponds with the expected capacity of Li_9Al_4 (2250 mAh/g) but not with the relative incremental capacities of Li_3Al_2 (1000 → 1500 mAh/g expected, 1000 → 2000 mAh/g observed) and Li_9Al_4 (1500 → 2250 mAh/g expected, 2000 → 2200 mAh/g observed). We are now performing ex- and in-situ studies to identify Li-Al phases and phase transitions. The bulk of the capacity shown in Figure 4 can likely be attributed to electrolyte breakdown and SEI formation at low voltages.

Results presented in Figures 2 and 4 demonstrate long term cycling of a Conflat cell at room temperature, and short term cycling at intermediate temperatures, respectively. Long term cycling of a Li-Si Conflat cell at intermediate temperatures (approximately 200 hours at each of 50°C, 75°C, and 100°C, and 250 hours at 120°C, for a total of ~850 hours) is presented in Figure 5. The Li-Si cell was cycled between 1.2 V and 50 mV vs. Li metal for a total of 6 cycles at each

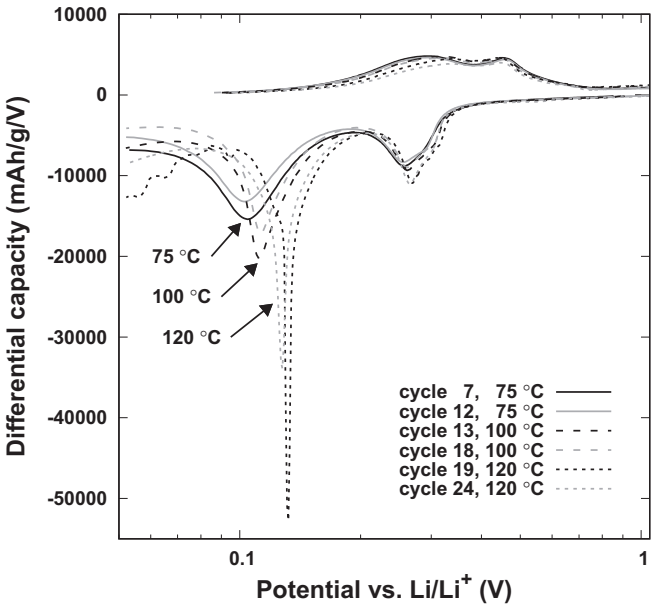

Figure 5. Differential capacity curves for a Li-Si cell cycled at various temperatures. The first (black) and last (gray) cycle at each of 75°C, 100°C, and 120°C are provided.

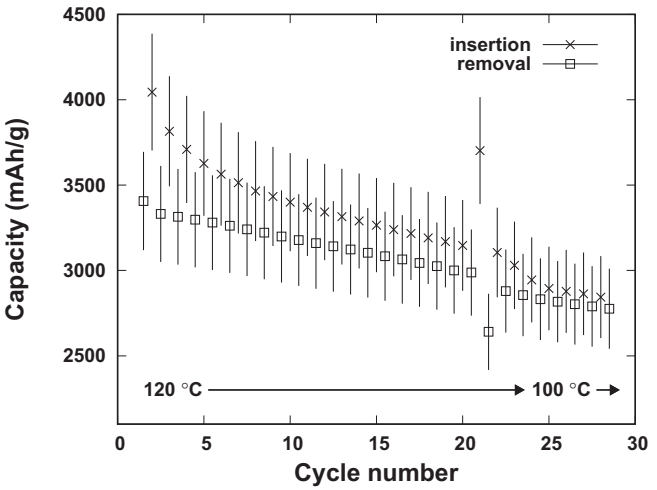

Figure 6. Capacity vs. cycle number for a Li-Si cell cycled at 120°C and 100°C as described in the text.

temperature; three cycles at a rate of C/7 followed by a galvanostatic intermittent titration (GITT) cycle and two additional cycles at a rate of C/7. Differential capacity curves from the first and last cycle at each temperature (other than at 50°C, which is very similar to data at 75°C) are shown. A logarithmic scale is used on the horizontal axis of Figure 5 for the sake of clarity. In general, differential capacity curves maintain their shape; the insertion peak near 0.1 V shifts to higher potential as the temperature increases, and then sharpens considerably when the cycling temperature is increased from 100°C to 120°C. The differential capacity peak at 130 mV at 120°C may correspond to the formation of $Li_{13}Si_4$, observed at 158 mV vs. Li metal at 415°C;[26] precise phase identification is ongoing, but the need and opportunity for low voltage electrochemical testing at intermediate temperatures is readily apparent.

Readers may note the change of electrolytes between data presented in Figure 3 (1 M $LiClO_4$ in EC:DEC, 90°C) and Figure 4 (1 M $LiN(SO_2CF_3)_2$ in EC:PC, 110 °C). Li-Al cells with 1 M $LiClO_4$ in EC:DEC 1:2 vol.:vol. electrolyte consistently failed (irregular voltage profiles, no Li removal capacity) when tested above ca. 100°C. 1 M $LiN(SO_2CF_3)_2$ in EC:PC 1:1 vol.:vol. is expected to be stable to higher temperatures.[27] Reversible cycling of Li-Al at 90°C as shown in Figure 3 also corresponded with increasing lithium consumption over time, even though the underlying reaction (Li + Al ↔ LiAl) did not change. Stable electrode phase transitions can thus be used to measure electrolyte breakdown and SEI formation as a function of time.

Results from a Li-Si conflat cell cycled between 1.2 V and 50 mV is presented in Figure 6. The first 23 cycles were performed at 120°C at a rate of C/10, followed by one GITT cycle, and then two additional cyles at a rate of C/10. Five subsequent C/10 cycles were performed at 100°C. Test duration was 600 hours at 120°C and 100 hours at 100°C. The first cycle insertion capacity was over 10,000 mAh/g and is not shown - a first cycle irreversible capacity of 7,000 mAh/g can only be reasonably attributed to electrolyte breakdown and SEI formation.

Lithium insertion and removal capacities shown in Figure 6 are in line with the reversible formation of Li_xSi ($x < 3.75$) at 3580 mAh/g.[28] Uncertainties in gravimetric capacity are primarily due to uncertainty in the thin film mass. Irreversible capacity drops quickly from 600 mAh/g on the second cycle to stabilize at approximately 150 mAh/g per cycle for cycles 10–20. High insertion capacity and low removal capacity during the 150 hour GITT cycle implies additional Li consumption and SEI growth. Once the operating temperature was reduced to 100°C, irreversible capacity quickly stabilized to approximately 70 mAh/g per cycle. Excluding the GITT cycle, lithium removal capacity faded by approximately 15 mAh/g per cycle.

An irreversible capacity of 150 mAh/g would quickly lead to capacity fade in a balanced cell; this cell was very unbalanced. However, the underlying capacity fade of the electrode material was an order of magnitude lower than the irreversible capacity. One can therefore use materials systems with known capacities (e.g. lithium-silicon) or distinct phase transitions (e.g. lithium-aluminum) as platforms for accelerated electrolyte degradation.

Cycling results above 120°C are not presented for two reasons. First, electrode and especially electrolyte failure was very pronounced at 120°C. Electrolyte breakdown was so significant that breakdown products become visible through the electrically insulating glass spacer, as shown in Figure 7. The glass spacer provides an opportunity for in-situ measurement of electrolyte breakdown products and SEI characterization. Conflat flanges with optical, infrared, or X-ray transparent windows are also commercially available. Second, 120°C is close to the melting point of Li (181°C); molten lithium cannot support any stack pressure. We are investigating the use of use prelithiated materials (e.g. LiAl foil) for testing electrode and electrolyte materials over a wide range of temperatures. Glass-to-metal Conflat

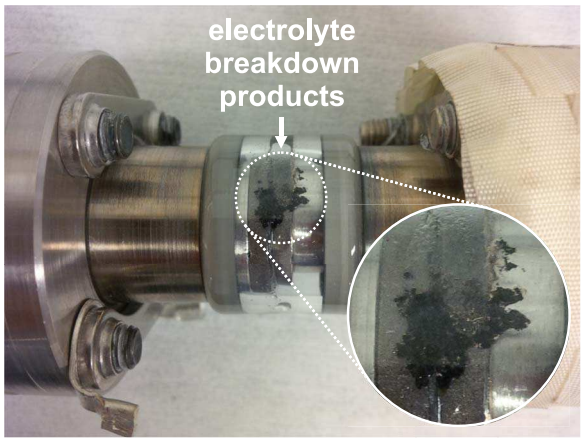

Figure 7. Image of Conflat cell after extended cycling at 110°C. Electrolyte breakdown products are visible (black, within white dashed circle, and inset solid circle).

cells without temperature-sensitive components have been tested up to 325°C, limited only by our available heater power and thermal insulation.

Conclusions

Glass-to-metal Conflat cells, introduced here, enable researchers to measure the performance (and limits) of electrode and electrolyte materials over a wide range of temperatures. Decoupling cell sealing and electrical isolation by using copper gaskets and glass-to-metal seals allowed for extended cycling at low, intermediate, and high temperatures with various electrolytes and negative electrode materials. Opportunities for metastable phase transitions and advanced electrolyte characterization (including direct observation of electrolyte breakdown products) are discussed.

Acknowledgments

Funding for this work was provided by National Research Council - Nanotechnology Research Centre. The authors thank P. Kalisvaart for thin film deposition and J. Pitters for helpful suggestions.

ORCID

Michael D. Fleischauer https://orcid.org/0000-0003-0725-2297

References

1. M. Jacoby, *Chemical & Engineering News*, **91**, 33 (2013).
2. X. Lin, M. Salari, L. M. R. Arava, P. M. Ajayan, and M. W. Grinsta, *Chem. Soc. Rev.*, **45**, 5848 (2016).
3. M.-T. F. Rodrigues, G. Babu, H. Gullapalli, K. Kalaga, F. N. Sayed, K. Kato, J. Joyner, and P. M. Ajayan, *Nature Energy*, **2**, 17108 (2017).
4. E. Talaie, P. Bonnick, X. Sun, Q. Pang, X. Liang, and L. F. Nazar, *Chemistry of Materials*, **29**, 90 (2017).
5. T. Marks, S. Trussler, A. J. Smith, D. Xiong, and J. R. Dahn, *Journal of The Electrochemical Society*, **158**, A51 (2011).
6. K. Periyapperuma, T. Tran, S. Trussler, D. Ioboni, and M. Obrovac, *Journal of The Electrochemical Society*, **161**, A2182 (2014).
7. R. S. Baldwin, NASA Technical Memorandum 216979/PART2 (2013).
8. A. Grenier, A. G. P. Gutierrez, H. Groult, and D. Dambournet, *Journal of Fluorine Chemistry*, **191**, 23 (2016).
9. M. N. Richard, I. Koetschau, and J. R. Dahn, *Journal of The Electrochemical Society*, **144**, 554 (1997).
10. A. Martinent, B. Le Gorrec, C. Montella, and R. Yazami, *Journal of Power Sources*, **97–98**, 83 (2001).
11. K. Y. Cheung, W. S. Lindsay, and D. J. Friedland, *Journal of The Electrochemical Society*, **2**, 1 (1985).
12. D. Guyomard and J.-M. Tarascon, *Journal of The Electrochemical Society*, **139**, 937 (1992).
13. F. Lepoivre, A. Grimaud, D. Larcher, and J.-M. Tarascon, *Journal of The Electrochemical Society*, **163**, A923 (2016).
14. A. Blyr, C. Sigala, G. Amatucci, D. Guyomard, Y. Chabre, and J.-M. Tarascon, *Journal of The Electrochemical Society*, **145**, 194 (1998).
15. D. Munoz-Rojas, J.-B. Leriche, C. Delacourt, P. Poizot, M. R. Palacín, and J.-M. Tarascon, *Electrochemistry Communicaitons*, **9**, 708 (2007).
16. F. Mestre-Aizpurua, S. Laruelle, S. Grugeon, J.-M. Tarascon, and M. R. Palacín, *Journal of Applied Electrochemistry*, **40**, 1365 (2010).
17. F. Mestre-Aizpurua, S. Hamelet, C. Masquelier, and M. Palacín, *Journal of Power Sources*, **195**, 6897 (2010).
18. J. Costard, M. Ender, M. Weiss, and E. Ivers-Tiffée, *Journal of The Electrochemical Society*, **164**, A80 (2017).
19. High Temperature Test Cells, https://el-cell.com/products/test-cells/high-temperature-test-cells/ Retreived: 2018-02-23.
20. R. Weidl, M. Schulz, M. Hofacker, H. Dohndorf, and M. Stelter, *AIP Conf. Proc.*, **1765**, 020004-1 (2016).
21. J. Cannarell and C. B. Arnold, *Journal of Power Sources*, **245**, 745 (2014).
22. M. D. Fleischauer, D. Tang, B. Gyenes, B. C. Olsen, and A. D. Johnson, submitted to *Review of Scientific Instruments* (2018).
23. T. R. Jow and C. C. Liang, *Journal of The Electrochemical Society*, **129**, 1429 (1982).
24. C. J. Wen, B. A. Boukamp, R. A. Huggins, and W. Weppner, *Journal of The Electrochemical Society*, **126**, 2258 (1979).
25. G. Oltean, C.-W. Tai, K. Edström, and L. Nyholm, *Journal of Power Sources*, **269**, 266 (2014).
26. C. J. Wen and R. A. Huggins, *Journal of Solid State Chemistry*, **37**, 271 (1981).
27. J. Dudley, D. Wilkinson, G. Thomas, R. LeVae, S. Woo, H. Blom, C. Horvath, M. Juzkow, B. Denis, P. Juric, P. Aghakian, and J. R. Dahn, *Journal of Power Sources*, **35**, 59 (1991).
28. M. N. Obrovac and L. Christensen, *Electrochemical and Solid-State Letters*, **7**, A93 (2004).